

An Aqueous Cooperative Assembly Route To Synthesize Ordered Mesoporous Carbons with Controlled Structures and Morphology

Fuqiang Zhang,[†] Yan Meng,[†] Dong Gu,[†] Yan Yan,[†] Zhenxia Chen,[†] Bo Tu,[†] and Dongyuan Zhao^{*,†,‡,§}

Department of Chemistry, Shanghai Key Laboratory of Molecular Catalysis and Innovative Materials, Key Laboratory of Molecular Engineering of Polymers, and Advanced Materials Laboratory, Fudan University, Shanghai 200433, People's Republic of China

Received June 16, 2006. Revised Manuscript Received July 27, 2006

A facile aqueous pathway has been demonstrated for the synthesis of ordered mesoporous carbon materials with hexagonal or cubic structures through the self-assembly of phenol/formaldehyde resols and triblock copolymer templates. Highly ordered mesoporous carbons FDU-16 with body-centered cubic structure (space group $Im\bar{3}m$) have been synthesized under a basic aqueous condition by using triblock copolymer Pluronic F127 ($EO_{106}PO_{70}EO_{106}$) as a template. Hydrocarbon (hexadecane or decane) can be used in the Pluronic P123 ($EO_{20}PO_{70}EO_{20}$) system as a swelling agent to synthesize highly ordered mesoporous carbons FDU-15 with 2-D hexagonal ($p6m$) structure. The pore size of FDU-15 can be tailored from 4.1 to 6.8 nm by simply varying the hydrocarbon molecules. Mesoporous carbon materials FDU-14 with bicontinuous cubic ($Ia\bar{3}d$) structure can be formed at a P123/phenol molar ratio higher than 0.04. A phase transformation from $Ia\bar{3}d$ to $p6m$ occurs as the P123/phenol ratio decreases. It is proposed that the cooperative assembly of resols and triblock copolymers driven by one-layer hydrogen bonds between the PEO segments and resols in aqueous solutions may favor the formation of mesostructures. Moreover, the morphology of the obtained mesoporous carbon materials can be controlled on the millimeter (1–5 mm) or micrometer (5–200 μm) scale. The simple aqueous route can give materials with a diversity of structures and morphologies, and this may offer the obtained materials very promising application prospects.

Introduction

Since their first discovery,^{1–2} mesoporous materials have attracted great interest for their variety in structure, morphology, and composition, which may result in wide potential applications in the fields of catalysis, separation, adsorption, etc. Commonly, mesoporous siliceous materials are synthesized by employing the cooperative assembly of inorganic precursors and amphiphilic surfactants through either a “hydrothermal” or an evaporation-induced self-assembly (EISA) pathway. To date, mesoporous silicates with a variety of structures, such as space groups $p6m$, $Im\bar{3}m$, $Ia\bar{3}d$, $Fm\bar{3}m$, $Pm\bar{3}n$, etc., have been successfully obtained.^{1–5} The meso-

structures can be well tailored by varying the amphiphilic surfactants with different hydrophilic/hydrophobic volume ratios or adding swelling agents or cotemplates. The diversity in the mesostructures may result in different properties for applications due to the derived different mass diffusion capacities. On the other hand, different application fields also have specific requirements of material morphologies; therefore, mesoporous materials with a variety of morphologies such as rods,^{6a} spheres,^{6b} single-crystal-like forms,^{6c,d} fibers,^{7a} films,^{7b,c} monoliths,^{7d} etc., have been obtained by varying the inorganic precursors or adding salts or small organic molecules.

Because of the amorphous pore wall feature, the framework compositions of mesoporous materials are variable. A high number of mesoporous nonsiliceous materials, such as metal oxides,^{8a–c} metal sulfides,^{8d} metal phosphates,^{8b} carbons,^{9–13} polymers,^{12–14} etc., have been prepared by either

* To whom correspondence should be addressed. Phone: 86-21-6564-2036. Fax: 86-21-6564-1740. E-mail: dyzhao@fudan.edu.cn.

[†] Department of Chemistry, Shanghai Key Laboratory of Molecular Catalysis and Innovative Materials.

[‡] Key Laboratory of Molecular Engineering of Polymers.

[§] Advanced Materials Laboratory.

- (1) (a) Kresge, C. T.; Leonowicz, M. E.; Roth, W. J.; Vartuli, J. C.; Beck, J. S. *Nature* **1992**, *359*, 710. (b) Beck, J. S.; Vartuli, J. C.; Roth, W. J.; Leonowicz, M. E.; Kresge, C. T.; Schmitt, K. D.; Chu, C. T. W.; Olson, D. H.; Sheppard, E. W.; McCullen, S. B.; Higgins, J. B.; Schlenker, J. L. *J. Am. Chem. Soc.* **1992**, *114*, 10834.
- (2) Inagaki, S.; Fukushima, Y.; Kuroda, K. *J. Chem. Soc., Chem. Commun.* **1993**, 680.
- (3) (a) Zhao, D. Y.; Feng, J. L.; Huo, Q. S.; Melosh, N.; Fredrickson, G. H.; Chmelka, B. F.; Stucky, G. D. *Science* **1998**, *279*, 548. (b) Zhao, D. Y.; Huo, Q. S.; Feng, J. L.; Chmelka, B. F.; Stucky, G. D. *J. Am. Chem. Soc.* **1998**, *120*, 6024.
- (4) (a) Ryoo, R.; Kim, J. M.; Ko, C. H.; Shin, C. H. *J. Phys. Chem.* **1996**, *100*, 17718. (b) Kleitz, F.; Choi, S. H.; Ryoo, R. *Chem. Commun.* **2003**, 2136.

- (5) Che, S.; Garcia-Bennett, A.E.; Yokoi, T.; Sakamoto, K.; Kunieda, H.; Terasaki, O.; Tatsumi, T. *Nat. Mater.* **2003**, *2*, 801.
- (6) (a) Zhao, D. Y.; Sun, J. Y.; Li, Q. Z.; Stucky, G. D. *Chem. Mater.* **2000**, *12*, 275. (b) Huo, Q. S.; Feng, J. L.; Schuth, F.; Stucky, G. D. *Chem. Mater.* **1997**, *9*, 14. (c) Che, S.; Sakamoto, Y.; Terasaki, O.; Tatsumi, T. *Chem. Mater.* **2001**, *13*, 2237. (d) Kim, J. M.; Kim, S. K.; Ryoo, R. *Chem. Commun.* **1998**, 259.
- (7) (a) Yang, P. D.; Zhao, D. Y.; Chmelka, B. F.; Stucky, G. D. *Chem. Mater.* **1998**, *10*, 2033. (b) Lu, Y. F.; Ganguli, R.; Drewien, C. A.; Anderson, M. T.; Brinker, C. J.; Gong, W. L.; Guo, Y. X.; Soyez, H.; Dunn, B.; Huang, M. H.; Zink, J. I. *Nature* **1997**, *389*, 364. (c) Zhao, D. Y.; Yang, P. D.; Melosh, N. A.; Feng, J. L.; Chmelka, B. F.; Stucky, G. D. *Adv. Mater.* **1998**, *10*, 1380. (d) Melosh, N. A.; Davidson, P.; Chmelka, B. F. *J. Am. Chem. Soc.* **2000**, *122*, 823.

a surfactant-assembly “soft” templating approach or a nanocasting “hard” template method from ordered mesoporous silica. Among these nonsiliceous materials, mesoporous carbon materials show very promising properties in catalysis, adsorption, and separation, even in electrochemistry, such as the electronic double-layer capacity (EDLC), in solar cells, in lithium ion batteries, etc., due to their electron-conducting frameworks, high surface areas, and large pores. The hard template route using ordered mesoporous silicates was first invented by Ryoo and co-workers,^{9a-c} which resulted in ordered mesoporous carbon materials with a variety of structures. The obtained mesoporous carbons possess reverse structures of mesoporous silicates. For example, CMK-3 material shows a hexagonal nanorod array, which is a reverse mesostructure of the silica template, the honeycomb-like SBA-15.^{9b} However, the key drawbacks of this hard template method are the extra steps required to prepare the scaffolds and the sacrificial use of not only the silica scaffolds themselves but also the surfactant templates; therefore, it is fussy and of a high cost, which may severely limit its applications.

For these reasons, great efforts have been made to explore a facile surfactant-assembly templating strategy to prepare mesoporous carbon materials with open-framework structures. More recently, researchers have demonstrated that the EISA of triblock copolymer and resols (phenol, resorcinol, or phloroglucinol/formaldehyde) is a method of high impact to synthesize ordered mesoporous carbon frameworks with $p6m$ and $Im\bar{3}m$ symmetry.¹⁰⁻¹² Although EISA is an appealing method for the preparation of films and monoliths, it is not a suitable pathway for industrial production due to the limitation of the batch size. Furthermore, uniaxial structural distortion is always observed for the mesoporous materials derived from the EISA method, and pore size tailoring is still a great challenge.^{8c}

The aqueous surfactant-assembly approach, which has been widely used in the synthesis of mesoporous silicates, is considered as an ideal method because it leads to highly ordered mesostructures with few defects, easily tailored pore sizes, and well-controlled morphologies. Compared to the EISA method, the aqueous route shows better reproducibility

and an unlimited fabrication batch size, which can meet the demands of industrial production well. On the basis of this consideration, we have recently developed an aqueous induced self-assembly strategy to prepare ordered mesoporous carbons with bicontinuous cubic structure.¹³ This aqueous approach for the synthesis of mesoporous carbons is as simple as that of mesoporous silicates and is considered as an industrially feasible method for the preparation of mesoporous carbons. However, it has not yet been proved to be efficacious to obtain mesoporous carbons with diversified structures such as $p6m$, $Im\bar{3}m$, etc.

In this paper, we report in detail a facile aqueous route to synthesize ordered mesoporous carbon frameworks with tailored mesostructures ($Im\bar{3}m$, $p6m$, and $Ia\bar{3}d$) and well-controlled morphologies by employing the organic-organic cooperative self-assembly of resols and triblock copolymers. Highly ordered mesoporous carbons FDU-16 with three-dimensional (3-D) body-centered cubic structure ($Im\bar{3}m$) were first obtained from the aqueous route by using triblock copolymer Pluronic F127 ($EO_{106}PO_{70}EO_{106}$) with a large PEO segment as a template. Hydrocarbons were employed as swelling agents in the organic-organic self-assembly, and 2-D hexagonal ($p6m$) mesoporous carbons FDU-15 were successfully obtained as a result. The pore size of the obtained FDU-15 can be tuned from 4.1 to 6.8 nm by varying the hydrocarbon molecules. Mesoporous carbons FDU-14 ($Ia\bar{3}d$) with bicontinuous cubic structure were synthesized by using Pluronic P123 ($EO_{20}PO_{70}EO_{20}$) as a template. A mesophase transformation from $Ia\bar{3}d$ to $p6m$ was observed as the P123/phenol ratio decreased. The morphology of the obtained carbons can be controlled on the micrometer scale (rods of 100–200 μm to particles of $\sim 5 \mu\text{m}$) or millimeter scale (small pellets of 1–5 mm). One-layer hydrogen bond interaction between resols and PEO segments was proposed to be the essential driving force that induces the organic-organic cooperative assembly.

Experiment Section

Chemicals. Triblock poly(ethylene oxide)-*b*-poly(propylene oxide)-*b*-poly(ethylene oxide) copolymers Pluronic P123 ($EO_{20}PO_{70}EO_{20}$, $M_{av} = 5800$) and Pluronic F127 ($EO_{106}PO_{70}EO_{106}$, $M_{av} = 12600$) were purchased from Aldrich. Hexadecane and decane were purchased from Fluka. Other chemicals were purchased from the Shanghai Chemical Co. All chemicals were used as received without further purification. Millipore water was used in all experiments.

Synthesis. Mesoporous carbon materials were synthesized by using triblock copolymer as a template and phenol/formaldehyde as a carbon precursor. First, 2.0 g (21 mmol) of phenol and 7.0 mL of formaldehyde solution (40 wt %, 100 mmol) were dissolved in 50 mL (5 mmol) of 0.1 M NaOH solution. Then the mixture was stirred at 70 °C for 30 min. A clear precursor solution (about 60 mL) was obtained, denoted as Solution-P.

FDU-16. For a typical synthesis of mesoporous carbon FDU-16, 4.4 g of F127 (~ 0.35 mmol) was dissolved in 50 mL of water. Then 60 mL of Solution-P was added to the above solution, and a clear solution was obtained. The solution turned dark red as it was stirred at 65 °C for about 3 h. Yellow precipitation was observed after about 24 h. The mixture was continuously stirred at 65 °C for an additional 72 h and then stirred at 70 °C for another 24 h.

- (8) (a) Antonelli, D. M.; Ying, J. Y. *Angew. Chem., Int. Ed. Engl.* **1995**, *34*, 2014. (b) Tian, B. Z.; Liu, X. Y.; Tu, B.; Yu, C. Z.; Fan, J.; Wang, L. M.; Xie, S. H.; Stucky, G. D.; Zhao, D. Y. *Nat. Mater.* **2003**, *2*, 159. (c) Tian, B. Z.; Liu, X. Y.; Solovyov, L. A.; Liu, Z.; Yang, H. F.; Zhang, Z. D.; Xie, S. H.; Zhang, F. Q.; Tu, B.; Yu, C. Z.; Terasaki, O.; Zhao, D. Y. *J. Am. Chem. Soc.* **2004**, *126*, 865. (d) Gao, F.; Lu, Q. Y.; Zhao, D. Y. *Adv. Mater.* **2003**, *15*, 739.
- (9) (a) Ryoo, R.; Joo, S. H.; Jun, S. J. *Phys. Chem. B* **1999**, *103*, 7743. (b) Jun, S.; Joo, S. H.; Ryoo, R.; Kruk, M.; Jaroniec, M.; Liu, Z.; Ohsumi, T.; Terasaki, O. *J. Am. Chem. Soc.* **2000**, *122*, 10712. (c) Joo, S. H.; Choi, S. J.; Oh, I.; Kwak, J.; Liu, Z.; Terasaki, O.; Ryoo, R. *Nature* **2001**, *412*, 169.
- (10) (a) Liang, C. D.; Hong, K. L.; Guiochon, G. A.; Mays, J. W.; Dai, S. *Angew. Chem., Int. Ed.* **2004**, *43*, 5785. (b) Liang, C. D.; Dai, S. J. *Am. Chem. Soc.* **2006**, *128*, 5316.
- (11) (a) Tanaka, S.; Nishiyama, N.; Egashira, Y.; Ueyama, K. *Chem. Commun.* **2005**, 2125. (b) Kosonen, H.; Valkama, S.; Nykanen, A.; Toivanen, M.; ten Brinke, G.; Ruokolainen, J.; Ikkala, O. *Adv. Mater.* **2005**, *18*, 201.
- (12) Meng, Y.; Gu, D.; Zhang, F. Q.; Shi, Y. F.; Yang, H. F.; Li, Z.; Yu, C. Z.; Tu, B.; Zhao, D. Y. *Angew. Chem., Int. Ed.* **2005**, *44*, 7053.
- (13) Zhang, F. Q.; Meng, Y.; Gu, D.; Yan, Y.; Yu, C. Z.; Tu, B.; Zhao, D. Y. *J. Am. Chem. Soc.* **2005**, *127*, 13508.
- (14) Rzaev, J.; Hillmyer, M. A. *J. Am. Chem. Soc.* **2005**, *127*, 13373.

The final product was collected by sedimentation separation and filtration, washed with water, and dried in air. The obtained sample was calcined at 500 and 800 °C for 3 h in a nitrogen flow to obtain mesoporous carbons FDU-16-500 and FDU-16-800, respectively. The heating rate was fixed at 1 °C/min.

FDU-15. For a typical synthesis of mesoporous carbon FDU-15, 1.6 g of hexadecane (7.1 mmol) or decane (11 mmol) was added to the solution of 3.2 g P123 (0.55 mmol) in 50 mL of water. The mixture was stirred at 40 °C for 5 h. A white mixture was obtained when 60 mL of Solution-P was added to the above mixture. The white mixture changed to dark red as it was stirred at 65 °C for about 3 h. Dark red precipitation was observed after the mixture was stirred at 65 °C for 24 h. The mixture was continuously stirred at 65 °C for an additional 72 h and then stirred at 70 °C for 24 h. The final products were collected and calcined as in the above procedure and assigned as FDU-15-*s*-350 and FDU-15-*s*-800, respectively, where *s* = C₁₆ when hexadecane was used and C₁₀ when decane was used.

FDU-14. For the typical synthesis of mesoporous carbon FDU-14, 4.8 g of P123 (0.83 mmol) was dissolved in 50 mL of water. Then 60 mL of Solution-P was added to the above mixture with stirring. A color change could be observed as mentioned above. The mixture was stirred at 65 °C for another 72 h and then at 70 °C for 24 h. The final products were collected and calcined as in the above procedure and assigned as FDU-14-350 and FDU-14-800, respectively.

All of the above syntheses can be carried out in a 10-fold quantity. For example, FDU-14 can be synthesized by dissolving 48 g of P123 in 500 mL of water and adding 600 mL of Solution-P. The obtained sample is assigned as FDU-14-L.

Characterization. Powder X-ray diffraction (XRD) patterns were recorded with a Bruker D4 powder X-ray diffractometer using Cu K α radiation (40 kV, 40 mA). The small-angle X-ray scattering (SAXS) measurements were taken on a Nanostar U small-angle X-ray scattering system (Bruker, Germany) using Cu K α radiation (40 kV, 35 mA). Nitrogen adsorption-desorption isotherms were measured with a Micromeritics Tristar 3000 analyzer at 77 K. Before the measurements, the samples were degassed at 200 °C in vacuum for 6 h. The Brunauer-Emmett-Teller (BET) method was utilized to calculate the specific surface areas. The pore size distributions were derived from the adsorption branches of the isotherms using the Kruk-Jaroniec-Sayari (KJS) method.¹⁵ The total pore volume, V_p , was estimated from the amount adsorbed at a relative pressure of 0.95. The unit cell parameters were calculated using the formulas $a = (\sqrt{2})d_{110}$, $a = 2d_{10}/\sqrt{3}$, and $a = (\sqrt{6})d_{211}$ for FDU-16, FDU-15, and FDU-14, respectively, where d_{110} , d_{10} , and d_{211} represent the d spacing values of the 110, 10, and 211 diffractions. The pore wall thicknesses were calculated from the formulas $t = a/3.0919 - D/2$,¹⁶ $t = a - D$, and $h = (\sqrt{3})a/2 - D$ ¹⁷ for FDU-14, FDU-15, and FDU-16, respectively, where a represents the unit cell parameter and D represents the KJS pore diameter. Transmission electron microscopy (TEM) experiments were conducted on a JEOL 2011 microscope operated at 200 kV. Scanning electron microscopy (SEM) images were taken with a Philips XL30 electron microscope operating at 20 kV. A thin gold film was sprayed on the sample before this characterization. Fourier transform infrared (FTIR) spectra were collected on a Nicolet Fourier spectrophotometer, using KBr pellets of the solid samples. The thermal decomposition behavior of the products was monitored

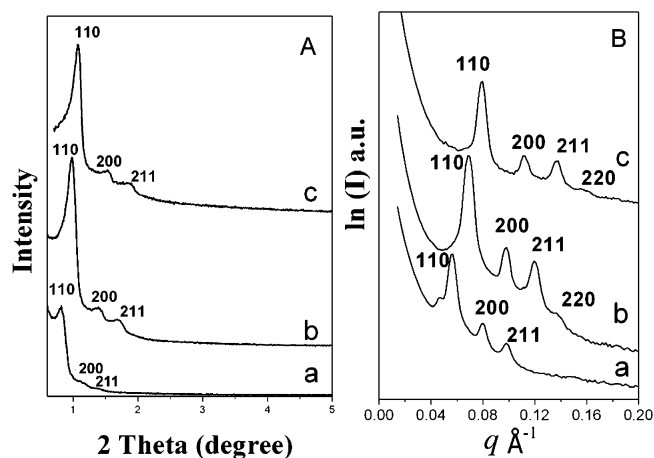


Figure 1. XRD (A) and SAXS (B) patterns of as-made FDU-16 (a), calcined FDU-16-500 (b), and calcined FDU-16-800 (c) prepared by using triblock copolymer F127 as a template.

using a Mettler Toledo TGA/SDTA851 analyzer from 25 to 900 °C under nitrogen with a heating rate of 5 °C/min. ¹³C solid-state NMR experiments were performed on a Bruker DSX300 spectrometer under conditions of cross polarization (CP) and magic angle sample spinning (MAS). The ¹³C solid-state NMR spectra were collected at room temperature with a frequency of 75 MHz (2 s recycle, 1 ms contact time) using adamantane as a reference. The C, H, and O contents were measured on a Vario EL III elemental analyzer.

Results

FDU-16. Mesoporous carbon FDU-16 can be synthesized in a basic aqueous solution by using triblock copolymer F127 as a template and phenol/formaldehyde resols as precursors. The powder XRD pattern (Figure 1A) of the as-made FDU-16 sample shows one diffraction peak at a 2θ of 0.8°. In addition, two weak and poor-resolved diffraction peaks can be observed. The low XRD intensity may be due to small contrast resulting from the similar densities of phenolic resins and triblock copolymers in the pore wall mesostructure. The SAXS pattern (Figure 1B) of as-made FDU-16 prepared by using F127 as a template in basic aqueous solution reveals three resolved diffraction peaks with a d spacing ratio of $1/(1/\sqrt{2})/(1/\sqrt{3})$, which can be indexed as 110, 200, and 211 diffractions of an ordered body-centered cubic mesostructure (space group $Im\bar{3}m$). After calcination at 500 °C in nitrogen, three well-resolved diffraction peaks can be clearly observed in the XRD pattern (Figure 1A), while one additional diffraction peak indexed as a 220 reflection can also be observed in the SAXS pattern (Figure 1B) for the FDU-16-500 sample, indicating a highly ordered cubic ($Im\bar{3}m$) mesostructure. Even after being calcined at 800 °C in N₂, the FDU-16-800 sample shows three well-resolved diffraction peaks of a cubic $Im\bar{3}m$ mesostructure in XRD and four diffraction peaks in the SAXS patterns (Figure 1), suggesting that the mesoporous carbon FDU-16 structure is thermally stable. The lattice parameter of as-made FDU-16 ($a = 15.4$ nm) decreased by 17.5% (FDU-16-500, $a = 12.7$ nm) after calcination at 500 °C and by 24.7% (FDU-16-800, $a = 11.6$ nm) after calcination at 800 °C (Table 1), suggesting that the framework suffers a large shrinkage in this process. An additional weak peak can be observed in the SAXS pattern

(15) (a) Kruk, M.; Jaroniec, M.; Sayari, A. *Langmuir* **1997**, *13*, 6267. (b) Kruk, M.; Jaroniec, M.; Ryoo, R.; Joo, S. H. *Chem. Mater.* **2000**, *13*, 1414.

(16) Ravikovitch, P. I.; Neimark, A. V. *Langmuir* **2000**, *16*, 2419.

(17) Ravikovitch, P. I.; Neimark, A. V. *Langmuir* **2002**, *18*, 1550.

Table 1. Lattice Size (a), Pore Diameter (D), Wall Thickness (t), BET Surface Area (S_{BET}), and Pore Volume (V_p) of Mesoporous Carbon Materials with Hexagonal or Cubic Structure

	symmetry	a (nm)	D (nm)	t (nm)	S_{BET} (m ² /g)	V_p (cm ³ /g)
FDU-16-500	$Im\bar{3}m$	12.7	3.5	7.5	670	0.34
FDU-16-800	$Im\bar{3}m$	11.6	3.2	6.8	1030	0.50
FDU-15-C ₁₆ -350	$p6m$	11.3	5.0	6.3	460	0.41
FDU-15-C ₁₀ -350	$p6m$	13.6	6.8	6.8	500	0.40
FDU-15-C ₁₆ -800	$p6m$	8.6	3.8	4.8	1040	0.55
FDU-15-C ₁₀ -800	$p6m$	10.9	4.1	6.8	750	0.40
FDU-14-350	$Ia\bar{3}d$	19.6	3.8	4.4	550	0.40
FDU-14-800	$Ia\bar{3}d$	15.4	2.8	3.6	1000	0.50
MP-1-350	$p6m^a$	10.2	4.1	6.1	450	0.30

^a A mixed mesophase of $p6m$ and $Ia\bar{3}d$ with a $p6m$ content of about 90%, which was roughly counted from the TEM measurements.

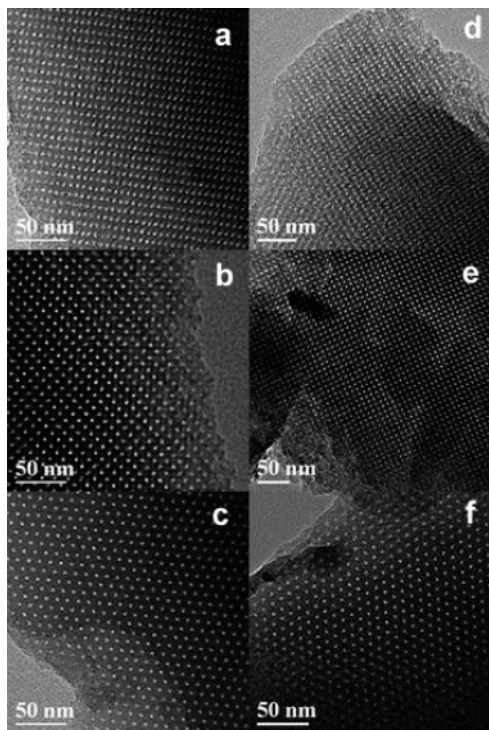


Figure 2. TEM images of FDU-16-500 (a–c) and FDU-16-800 (d–f) viewed along the [110] (a, d), [100] (b, e), and [111] (c, f) directions. FDU-16-500 and FDU-16-800 were prepared by using triblock copolymer F127 as a template in a basic aqueous solution and calcined at 500 and 800 °C in a N₂ flow.

of as-made FDU-16, which may be assigned to a minor $Im\bar{3}m$ phase (the same mesostructure) with a larger lattice size caused by inhomogeneous precipitation. After calcination, the difference between the d_{110} spacing values of the $Im\bar{3}m$ phases with different lattice sizes may decrease for structural shrinkage (the larger the d spacing is, the larger the shrinkage is), which will result in the merging of diffraction peaks. Thus, the additional diffraction peak is not resolved in the SAXS pattern of calcined FDU-16 samples. The lattice size (15.4 nm) of as-made FDU-16 from the present aqueous method is smaller compared to that of the as-made FDU-16 ($a = 18.1$ nm) from the EISA method, while the structural shrinkage (24.7%) after calcination at 800 °C is very similar to that from the EISA method (24%).¹²

The TEM images (Figure 2a–c) of FDU-16-500 reveal typical patterns of a body-centered cubic structure viewed along the [110], [100], and [111] directions, further confirm-

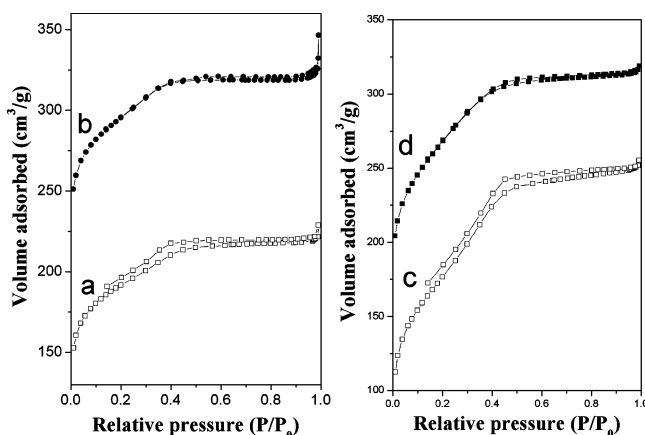


Figure 3. Nitrogen sorption isotherms of FDU-16-500 (a), FDU-16-800 (b), FDU-14-350 (c), and FDU-14-800 (d). FDU-16-500 and FDU-16-800 were prepared by using triblock copolymer F127 as a template in a basic aqueous solution and calcined at 500 and 800 °C in N₂. FDU-14-350 and FDU-14-800 were prepared by using triblock copolymer P123 as a template and calcined at 350 and 800 °C in a N₂ flow.

ing a cubic $Im\bar{3}m$ mesostructure. After calcination at 800 °C, the obtained sample FDU-16-800 also displays typical morphologies viewed along the [110], [100], and [111] directions (Figure 2d–f), suggesting that the cubic FDU-16 mesostructure is stable. The cell parameters calculated from the TEM images are in good agreement with those from XRD and SAXS, while the structural shrinkage can be directly concluded from the TEM images.

Both FDU-16-500 and FDU-16-800 show type IV sorption isotherms (Figure 3a,b) with clear nitrogen condensation steps. The adsorption and desorption branches of FDU-16-500 are not close at low relative pressure, suggesting a typical sorption behavior of polymer materials.¹⁸ It can be calculated from the nitrogen adsorption branch that FDU-16-500 has a pore size of 3.5 nm, a BET surface area of 670 m²/g, and a pore volume of 0.34 cm³/g (Table 1). During the carbonization process from 500 to 800 °C, the pore size of FDU-16 decreases from 3.5 to 3.2 nm, a decrease of about 8.6%, while the BET surface area and pore volume increase to 1030 m²/g and 0.50 cm³/g, respectively. The wall thickness calculated on the basis of the reported method¹⁷ decreases from 7.5 to 6.8 nm after this process. Our results show that when the calcination temperature is lower than 500 °C, the mesoporosity of FDU-16 can not be generated, which may be due to the small pore entrance in FDU-16.

Ordered mesoporous carbons FDU-16 can be synthesized at a relatively wide range of F127 concentration with a reactant composition (molar ratio) of F127/pheol/HCHO/NaOH/H₂O = $y/2.1/10/0.50/580$, where $y = 0.035, 0.040,$ and 0.048 , denoted as FDU-16- y . All the materials were calcined at 500 °C to generate mesoporous carbons with good regularity, which could make the structural characterization easy. Three well-resolved diffraction peaks indexed as 110, 200, and 211 of $Im\bar{3}m$ symmetry can be observed in the XRD patterns (Figure 4A) for each sample, indicating the highly ordered body-centered cubic mesostructure.

(18) McKeown, N. B.; Budd, P. M.; Msayib, K. J.; Ghanem, B. S.; Kingston, H. J.; Tattershall, C. E.; Makhseed, S.; Reynolds, K. J.; Fritsch, D. *Chem.—Eur. J.* **2005**, *11*, 2610.

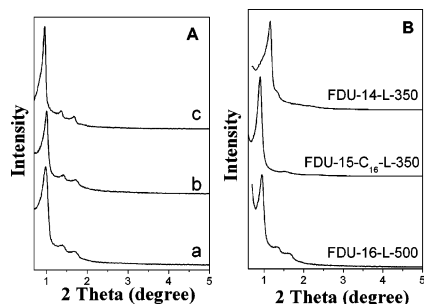


Figure 4. (A) XRD patterns of FDU-16-y-500 prepared with a reactant composition of F127/phenol/HCHO/NaOH/H₂O = y/2.1:1:10:0.50:580, y = 0.035 (a), 0.040 (b), and 0.048 (c), and calcined at 350 °C in a N₂ flow. (B) XRD patterns of FDU-16-L-500, FDU-15-C₁₆-350, and FDU-14-L-350, which were prepared in larger quantities.

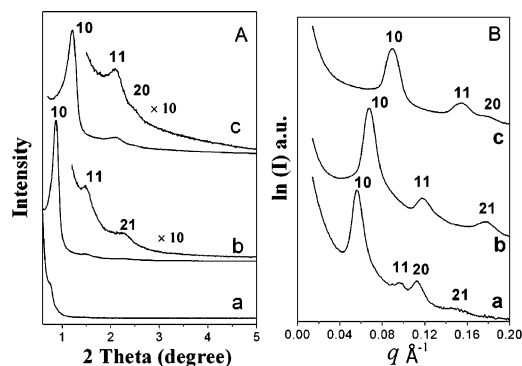


Figure 5. XRD patterns (A) and SAXS (B) patterns of as-made FDU-15-C₁₆ (a), calcined FDU-15-C₁₆-350 (b), and calcined FDU-15-C₁₆-800 (c). FDU-15-C₁₆ was prepared by using triblock copolymer P123 as a template and hexadecane as a swelling agent and calcined at 350 and 800 °C in a N₂ flow.

FDU-15. For the synthesis of mesoporous silicate materials in aqueous conditions using triblock copolymers as templates, some hydrocarbon molecules such as 1,3,5-trimethylbenzene (TMB)^{19–20} and hexane, nonane, etc.^{21,22} can be used as pore size swelling agents. The hydrocarbon molecules can interact with the hydrophobic PPO segment of the triblock copolymers; as a result, the lattice is enlarged or the phase transition occurs. By using hexadecane as a swelling agent, mesoporous carbon FDU-15-C₁₆ was synthesized under an aqueous condition with a reactant molar ratio of P123/hexadecane/phenol/HCHO/NaOH/H₂O = 0.055/0.71/2.1/10/0.50/580. Similar to that of FDU-16, the XRD pattern (Figure 5A-a) of as-made FDU-15-C₁₆ shows only one poorly resolved shoulder peak, while the SAXS pattern (Figure 5B-a) reveals four resolved diffraction peaks which can be indexed as 10, 11, 20, and 21 reflections associated with an ordered 2-D hexagonal *p6m* mesostructure. After calcination at 350 °C, the XRD pattern of FDU-15-C₁₆-350 shows a strong and narrow 10 reflection peak (*d* spacing 9.8 nm) and two well-

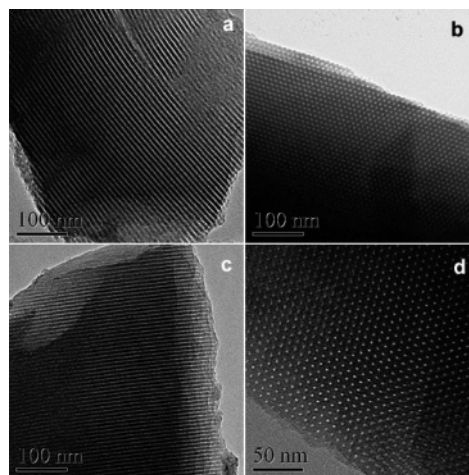


Figure 6. TEM images of FDU-15-C₁₆-350 (a, b) and FDU-15-C₁₆-800 (c, d) viewed along the [110] (a, c) and [001] (b, d) directions.

resolved 11 and 21 reflection peaks of *p6m* symmetry, indicating a highly ordered 2-D hexagonal structure. The SAXS pattern of FDU-15-C₁₆-350 also displays intense resolved 10, 11, and 21 reflection peaks. After calcination at 800 °C, the obtained mesoporous carbon FDU-15-C₁₆-800 reveals typical 10, 11, and 20 reflection peaks of *p6m* symmetry in XRD and SAXS patterns, suggesting good thermal stability. It should be noticed that the 20 diffraction peak is not resolved in the SAXS pattern of FDU-15-C₁₆-350, while that of FDU-15-C₁₆-800 is well resolved, probably because it is too close to the wide 11 reflection and merged in it. After calcination at 800 °C the reflection peaks shift to high angle due to the framework shrinkage; thus, the 11 and 20 reflection peaks are separated greatly. The lattice parameters of FDU-15-C₁₆, FDU-15-C₁₆-350, and FDU-15-C₁₆-800 calculated from the SAXS patterns are 13.0, 11.3, and 8.6 nm, respectively, suggesting a large shrinkage. Compared to FDU-16 (shrinkage of 24.7%), FDU-15-C₁₆ shows a larger structural shrinkage of 33.8% after the carbonization process at 800 °C. Our results show that FDU-15-C₁₆ can be synthesized with a reactant molar ratio of P123/hexadecane/phenol/HCHO/NaOH/H₂O = (0.048–0.055)/(0.35–1.4)/2.1/10/0.50/580.

The TEM images of FDU-15-C₁₆-350 show typical patterns viewed along the [110] and [001] directions (Figure 6a,b). No other mesophase can be observed, implying that the ordered 2-D hexagonal mesostructure is a pure phase. After calcination at 800 °C, typical patterns along the [110] (Figure 6c) and [001] (Figure 6d) directions of the 2-D hexagonal mesostructure can be observed in the TEM images, suggesting that FDU-15-C₁₆ is thermally stable and no phase evolution occurs during the calcination.

The nitrogen sorption isotherms of both FDU-15-C₁₆-350 and FDU-15-C₁₆-800 show representative type IV curves with sharp capillary condensation steps (Figure 7a,b). The adsorption and desorption branches of FDU-15-C₁₆-350 are not close at low relative pressure, which may be related to the sorption behavior of polymer materials. It can be calculated from the nitrogen adsorption branch that FDU-15-C₁₆-350 has a pore size of 5.0 nm, a BET surface area of 460 m²/g, and a pore volume of 0.41 cm³/g, while FDU-15-C₁₆-800 possesses a pore size of 3.8 nm, a BET surface

- (19) (a) Schmidt-Winkel, P.; Lukens, W. W.; Zhao, D. Y.; Yang, P. D.; Chmelka, B.F.; Stucky, G. D. *J. Am. Chem. Soc.* **1999**, *121*, 254. (b) Schmidt-Winkel, P.; Lukens, W. W.; Yang, P. D.; Margolese, D. I.; Lettow, J. S.; Ying, J. Y.; Stucky, G. D. *Chem. Mater.* **2000**, *12*, 686.
- (20) (a) Fan, J.; Yu, C. Z.; Gao, F.; Lei, J.; Tian, B. Z.; Wang, L. M.; Luo, Q.; Tu, B.; Zhou, W. Z.; Zhao, D. Y. *Angew. Chem., Int. Ed.* **2003**, *42*, 3146. (b) Chen, D. H.; Li, Z.; Wan, Y.; Tu, X. J.; Shi, Y. F.; Chen, Z. X.; Shen, W.; Yu, C. Z.; Tu, B.; Zhao, D. Y. *J. Mater. Chem.* **2006**, *16*, 1511.
- (21) Sun, J. M.; Zhang, H.; Ma, D.; Chen, Y. Y.; Bao, X. H.; Klein-Hoffmann, A.; Pfander, N.; Su, D. S. *Chem. Commun.* **2005**, 5343.
- (22) El-Safty, S. A.; Hanaoka, T. *Chem. Mater.* **2004**, *16*, 384.

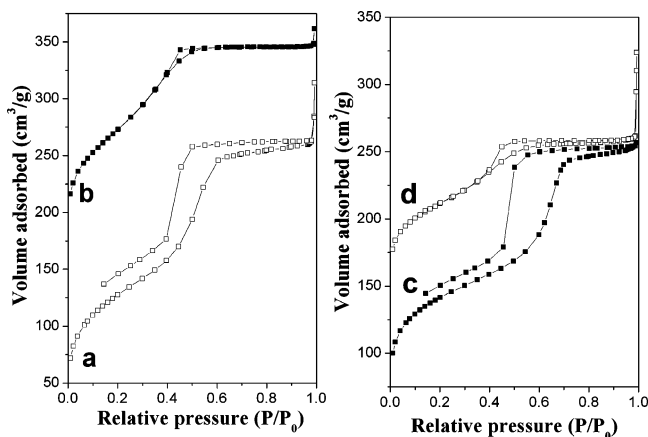


Figure 7. Nitrogen sorption isotherms of 2-D hexagonal FDU-15-C₁₆-350 (a), FDU-15-C₁₆-800 (b), FDU-15-C₁₀-350 (c), and FDU-15-C₁₀-800 (d). FDU-15-C₁₆-350 and FDU-15-C₁₆-800 were prepared by using P123 as a template and hexadecane as a swelling agent and calcined at 350 and 800 °C in a N₂ flow. FDU-15-C₁₀-350 and FDU-15-C₁₀-800 were prepared by using P123 as a template and decane as a swelling agent and calcined at 350 and 800 °C in a N₂ flow.

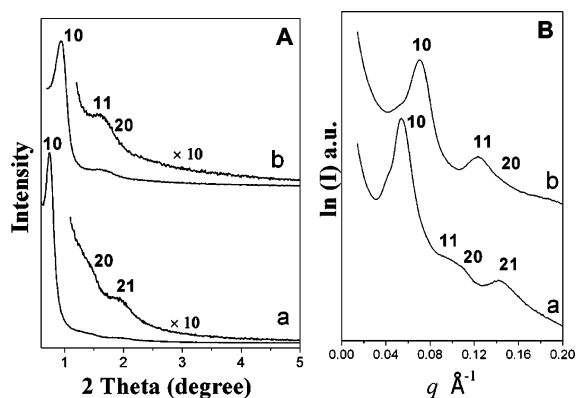


Figure 8. XRD (A) and SAXS (B) patterns of FDU-15-C₁₀-350 (a) and FDU-15-C₁₀-800 (b) prepared by using triblock copolymer P123 as a template and decane as a swelling agent and calcined at 350 and 800 °C in a N₂ flow.

area of ~ 1040 m²/g, and a pore volume of ~ 0.55 cm³/g (Table 1).

By using decane, a shorter chain hydrocarbon, as a swelling agent, 2-D hexagonal FDU-15-C₁₀ with a larger lattice compared to FDU-15-C₁₆ can be prepared with a reactant molar ratio of P123/decane/phenol/HCHO/NaOH/H₂O = 0.055/1.1/2.1/10/0.50/580. The XRD pattern of FDU-15-C₁₀-350 shows three diffraction peaks associated with the 10, 20, and 21 reflections of the 2-D hexagonal *p6m* mesostructure (Figure 8A-a). The SAXS pattern (Figure 8B-a) with four resolved diffraction peaks indexed to the 10, 11, 20, and 21 reflections further confirms a hexagonal *p6m* mesostructure. After calcination at 800 °C, the XRD pattern (Figure 8A-b) shows one intense diffraction peak and two weak peaks, while the SAXS pattern (Figure 8B-b) of FDU-15-C₁₀-800 reveals 10, 11, and 20 reflection peaks, further suggesting good thermal stability. Nevertheless, the reflection peaks in the SAXS patterns of FDU-15-C₁₀ are weaker and wider compared to those of FDU-15-C₁₆, suggesting a poorer regularity. The lattice parameters calculated from the SAXS patterns are 13.6 and 10.9 nm for FDU-15-C₁₀-350 and FDU-15-C₁₀-800, respectively, which are larger than those for FDU-15-C₁₆-350 and FDU-15-C₁₆-800 (Table 1). The nitro-

gen sorption isotherms (Figure 7c,d) of FDU-15-C₁₀-350 and FDU-15-C₁₀-800 show type IV curves with steep condensation steps at higher relative pressure ($P/P_0 = 0.3-0.5$), suggesting a uniform mesopore distribution. The pore sizes calculated by the KJS model are 6.8 and 4.1 nm for FDU-15-C₁₀-350 and FDU-15-C₁₀-800, respectively, which are a little larger than those for FDU-15-C₁₆-350 and FDU-15-C₁₆-800 (Table 1). These results suggest that smaller hydrocarbon molecules have a stronger interaction with the copolymer templates and show larger pores and a larger lattice parameter.²³ It should be noticed here that the main desorption occurs at a low relative pressure range (0.45–0.5), which is not a typical hysteresis loop of cylindrical pores, suggesting that some pore distortion may exist in FDU-15-C₁₀-350 and partially block the channels.

When hydrocarbon molecules smaller than decane, such as TMB, heptane, hexane, etc., were used as swelling agents in this system, only a disordered mesostructure could be obtained. Without using a swelling agent, mesoporous carbons with a pure 2-D hexagonal mesophase cannot be obtained under aqueous synthesis conditions. For example, a mesoporous material (MP-1) was obtained with a reactant molar ratio of 0.055 P123/2.1 phenol/10 HCHO/0.5 NaOH/580 H₂O without addition of any swelling agent. The SAXS pattern (Figure 11a) of MP-1-350 shows two broad diffraction peaks with a *d* spacing ratio of about $1/(1/\sqrt{3})$, suggesting a probable hexagonal *p6m* symmetry. The TEM characterization shows that MP-1-350 obtained after calcination at 350 °C in nitrogen is mainly composed of a 2-D hexagonal *p6m* mesostructure, while a minor phase of *Ia3d* symmetry is also observed.

FDU-14. A bicontinuous cubic *Ia3d* mesoporous carbon structure (FDU-14) can also be synthesized in a basic aqueous solution by using triblock copolymer P123 as a template.¹³ For the systematization, here we report a detailed synthesis of FDU-14. Interestingly, a phase transition from cubic *Ia3d* to hexagonal *p6m* is found in the P123 system.

The XRD and SAXS patterns of mesoporous carbon FDU-14 prepared with a reactant molar ratio of P123/phenol/HCHO/NaOH/H₂O = 0.083/2.1/10/0.50/580 are shown in Figure 9. Two poorly resolved diffraction peaks can be observed in the XRD pattern of as-made FDU-14, while six resolved diffraction peaks, indexed as 211, 220, 321, 400, 420, and 332 reflections of a bicontinuous cubic *Ia3d* mesostructure, are shown in the SAXS pattern. After calcination at 350 °C, four well-resolved peaks, indexed as 211, 220, 420, and 332 reflections, can clearly be observed in the XRD pattern of FDU-14-350, suggesting a highly ordered bicontinuous cubic mesostructure. The mesostructure can be further confirmed by the SAXS pattern with six well-resolved diffraction peaks. After calcination at 800 °C, the *Ia3d* mesostructure is well retained, suggesting good thermal stability. However, the reflection peaks shift to higher angle and become weaker and wider, indicating that the structure shrank and the regularity decreased. It is worth noticing that a weak 110 reflection peak associated with the *I432* symmetry can be observed in the SAXS patterns (Figure 9B-

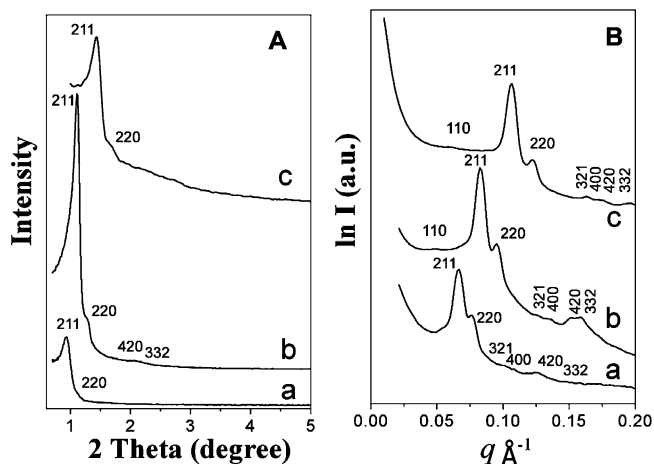


Figure 9. XRD (A) and SAXS (B) patterns of ordered bicontinuous cubic FDU-14 prepared by using P123 as a template in a basic aqueous solution: (a) as-made FDU-14 and (b) FDU-14-350 calcined at 350 °C and (c) FDU-14-800 calcined at 800 °C in a N₂ flow.

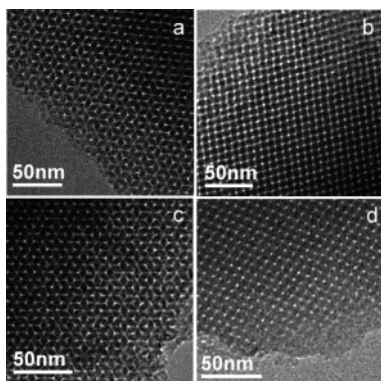


Figure 10. TEM images of FDU-14-350 (a, b) and FDU-14-800 (c, d) viewed along the [111] (a, c) and [531] (b, d) directions.

b,c), suggesting a structural defect. FDU-14-350 and FDU-14-800 possess fundamentally related structures in spite of the shrinkage. The lattice shrinkage calculated from XRD data is 32.6% for FDU-14-800, which is similar to that (33.8%) of FDU-15-C₁₆-800 and larger than that (24.7%) of FDU-16, suggesting that body-centered cubic mesostructure FDU-16 is more stable than FDU-14 (*Ia* $\bar{3}$ *d*) and FDU-15 (*p*6*m*). The TEM images of FDU-14-350 and FDU-14-800 (Figure 10) show typical morphologies of a bicontinuous cubic *Ia* $\bar{3}$ *d* structure viewed along the [111] and [531] directions, further confirming an ordered *Ia* $\bar{3}$ *d* mesostructure. It should be mentioned that no image for *I*4₁32 symmetry was observed during our TEM measurements, suggesting that most domains of the FDU-14 structure are of *Ia* $\bar{3}$ *d* symmetry. The nitrogen sorption isotherms of both FDU-14-350 and FDU-14-800 (Figure 3c,d) are type IV curves with very clear capillary condensation steps, suggesting uniform mesopore distributions. FDU-14-350 has a pore size of 3.8 nm and a BET surface area of ~550 m²/g (Table 1). Compared with FDU-14-350, FDU-14-800 has a smaller pore size of 2.8 nm and a higher BET surface area of ~1000 m²/g, suggesting structural contraction and generation of micropores. Among all the mesoporous carbon structures (Table 1), FDU-14 shows the smallest pore sizes, in agreement with the structural shrinkages.

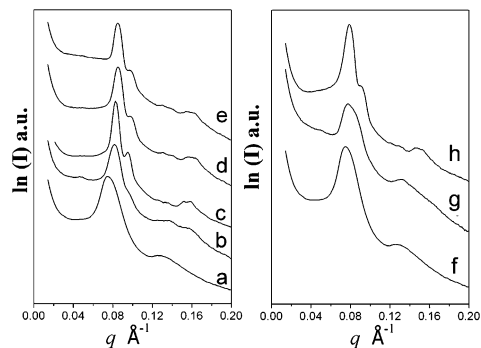


Figure 11. (A) SAXS patterns of mesoporous polymers prepared with a reactant molar ratio of P123/phenol/HCHO/NaOH/H₂O = *x*/2.1/10/0.50/580, where *x* = 0.055 (a), 0.069 (b), 0.083 (c), 0.097 (d), and 0.11 (e). (B) SAXS patterns of mesoporous polymers obtained with a reactant molar ratio of P123/phenol/HCHO/NaOH/H₂O = 0.055/2.1*y*/10*y*/0.50*y*/580, where *y* = 1 (f), 0.8 (g), and 0.66 (h). All samples were calcined at 350 °C in a N₂ flow for 3 h.

SAXS patterns (Figure 11) show that the synthesis process is greatly influenced by the P123/phenol ratio. When the phenol concentration is fixed, the samples obtained at a relatively high P123/phenol ratio (P123/phenol/HCHO/NaOH/H₂O = *x*/2.1/10/0.50/580, *x* = 0.083, 0.097, and 0.11, P123/phenol molar ratios of 0.040, 0.046, and 0.052, respectively) show typical SAXS (Figure 11c–e) patterns assigned to a bicontinuous cubic *Ia* $\bar{3}$ *d* mesostructure. It is noteworthy that the samples synthesized at low P123/phenol ratios (0.026 and 0.033) display broad and poorly resolved diffraction peaks (Figure 11a,b). With the aid of TEM, these samples possess a mixed mesophase of *p*6*m* and *Ia* $\bar{3}$ *d*. The ratio of the two phases in the samples was roughly counted from the TEM measurements. The content of the *p*6*m* mesophase increases dramatically from about 10% to 90% with a decrease of the P123/phenol ratio from 0.033 to 0.026. When the P123 concentration is fixed at a relatively low value of ~2.8 wt % (P123/phenol/HCHO/NaOH/H₂O = 0.055/2.1*y*/10*y*/0.50*y*/580), three samples are synthesized by varying the P123/phenol ratio as 0.040, 0.033, and 0.026 (*y* = 0.66, 0.8, and 1, respectively). The SAXS patterns show that the same trend of phase evolution associated with the P123/phenol molar ratio can be concluded. The SAXS pattern (Figure 11h) of the sample prepared with a P123/phenol molar ratio of 0.040 shows typical reflection peaks of an ordered *Ia* $\bar{3}$ *d* structure, while the samples synthesized with P123/phenol ratios of 0.033 and 0.026 show broader diffraction peaks (Figure 11 g,h). Combining the TEM results, the latter two samples are mixed phases of *Ia* $\bar{3}$ *d* and *p*6*m*. The content of the *p*6*m* mesostructure increases greatly as the P123/phenol molar ratio decreases. On the basis of these results, it is clearly shown that the P123/phenol ratio is one of the fundamental factors that induce the phase transition. Without addition of hydrocarbon molecules, a pure (100%) hexagonal *p*6*m* mesophase could not be obtained; the highest content of the *p*6*m* phase is about ~90% on the basis of our observations (MP-1-350).

Another unique feature of aqueous synthesis is that it can be carried out in a larger quantity. FDU-16-L-500, FDU-15-C₁₆-L-350, and FDU-14-L-350 were prepared in a 10 times larger batch. The XRD patterns of FDU-16-L-500, FDU-15-C₁₆-L-350, and FDU-14-L-350 (Figure 4B) are in

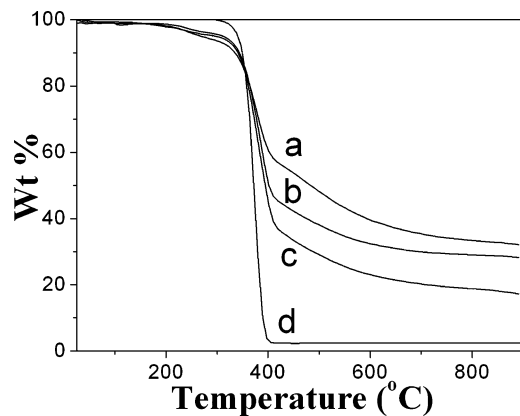


Figure 12. TGA curves of as-made FDU-16 (a), as-made FDU-15-C₁₆ (b), as-made FDU-14 (c), and Pluronic F127 (d) in a nitrogen flow with a heating rate of 5 °C/min.

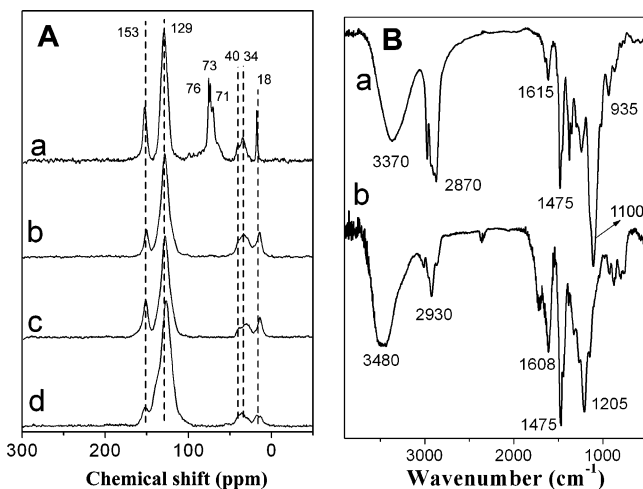


Figure 13. ¹³C solid-state NMR spectra (A) and FTIR spectra (B) of as-made FDU-14 (a), FDU-14-350 (b), FDU-15-C₁₆-350 (c), and FDU-16-500 (d).

good agreement with those of the samples of small quantity, indicating that the current aqueous synthesis of mesoporous carbon can be performed in a much larger batch.

Frameworks. The TGA curves for all as-made samples prepared from the aqueous cooperative assembly route by using triblock copolymers as templates are shown in Figure 12. Each sample displays significant weight loss from 350 to 400 °C in nitrogen. In this temperature range, the as-made FDU-16, FDU-15-C₁₆, and FDU-14 show large weight losses of about 40, 55, and 61 wt %, respectively (Figure 12a–c), which agree well with that of Pluronic triblock copolymer (Figure 12d), suggesting that the templates can be removed after calcination at 350 °C. As the mesophase transformed from *Im* $\bar{3}m$ to *p6m* and *Ia* $\bar{3}d$, the hydrophilic/hydrophobic volume ratio decreased while the surfactant weight ratio increased at the same time. Thus, the weight loss of as-made FDU-16 (40%) is less than those of FDU-15-C₁₆ (55%) and FDU-14 (61%). The ¹³C solid-state NMR spectrum (Figure 13A-a) of as-made FDU-14 shows three resonance signals at chemical shifts of 71, 73, and 76 ppm, which are assigned to the carbon atoms connected with O atoms, –CH–, and –CH₂– in triblock copolymer P123.^{24a} In addition, two strong signals with chemical shifts of 153 and 129 ppm are also observed, which are attributed to the OH-substituted,



Figure 14. Photographs of as-made FDU-14 (a), FDU-14-350 (b), FDU-14-800 (c), as-made FDU-15-C₁₆ (d), FDU-15-C₁₆-350 (e), and FDU-15-C₁₆-800 (f).

aromatic (except H-substituted) carbons of phenolic resins. The peaks between 34 and 40 ppm are assigned to the methylene carbon.^{24b} These results suggest a triblock copolymer/phenolic resin mesostructure. After calcination at 350 °C in nitrogen, only signals from the phenolic resin can be observed, indicating that most of the P123 is decomposed and a phenolic resin framework is formed. The ¹³C NMR spectra of FDU-15-C₁₆-350 (Figure 13A-c) and FDU-16-500 (Figure 13A-d) also display typical resonance signals of phenolic resins, suggesting the formation of phenolic resin frameworks. Elemental analysis results show that all the as-made samples obtained in the aqueous synthesis process are composed of C, H, and O elements. The C/H/O molar ratios of FDU-14-350, FDU-15-C₁₆-350, and FDU-16-500 are 6.5/4.2/1, 6.3/4.2/1, and 7/4/0.75, respectively, further confirming their phenolic resin polymer frameworks. FDU-14-800, FDU-15-C₁₆-800, and FDU-16-800 samples show a carbon content of over 90 wt %, suggesting that the as-made composites can be directly transferred to carbon frameworks after calcination at 800 °C in nitrogen. The composition variation can also be confirmed in the FTIR (Figure 13B) spectra of FDU-14 and FDU-14-350. The typical absorption of P123 at 1100 cm⁻¹ disappears after calcination at 350 °C, and only those bands from phenolic resin are observed, further confirming the decomposition of P123 at 350 °C.

Morphology. The present aqueous route has displayed its great advantages in the successful preparation of highly ordered mesoporous carbon materials with a variety of structures (*p6m*, *Im* $\bar{3}m$, and *Ia* $\bar{3}d$). Moreover, another unique feature of the aqueous route is that the morphology can be controlled on the scale of millimeters or micrometers. The photograph in Figure 14a shows that the as-made FDU-14 is composed of irregular pellets on the millimeter scale (about 3–5 mm). After calcination, the pellet-like morphology is well retained, although an obvious shrinkage (30–60%) in size occurs (Figure 14b,c). FDU-14-350 has a pellet size of 2–4 mm and FDU-14-800 a pellet size of 1–2 mm. Compared to FDU-14, as-made FDU-15-C₁₆ prepared by using the same copolymer P123 as a template in aqueous solution also shows pellet-like morphology (Figure 14d–f)

(24) (a) Yang, C. M.; Zibrowius, B.; Schmidt, W.; Schuth, F. *Chem. Mater.* **2003**, *15*, 3739. (b) GrenierLoustalot, M. F.; Larroque, S.; Grenier, P. *Polymer* **1996**, *37*, 639.

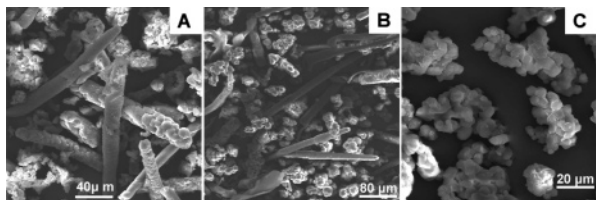


Figure 15. SEM images of as-made FDU-16 obtained with a molar ratio of F127/phenol/HCHO/NaOH/H₂O = $y/2.1/10/0.50/580$, $y = 0.035$ (A), 0.040 (B), and 0.048 (C).

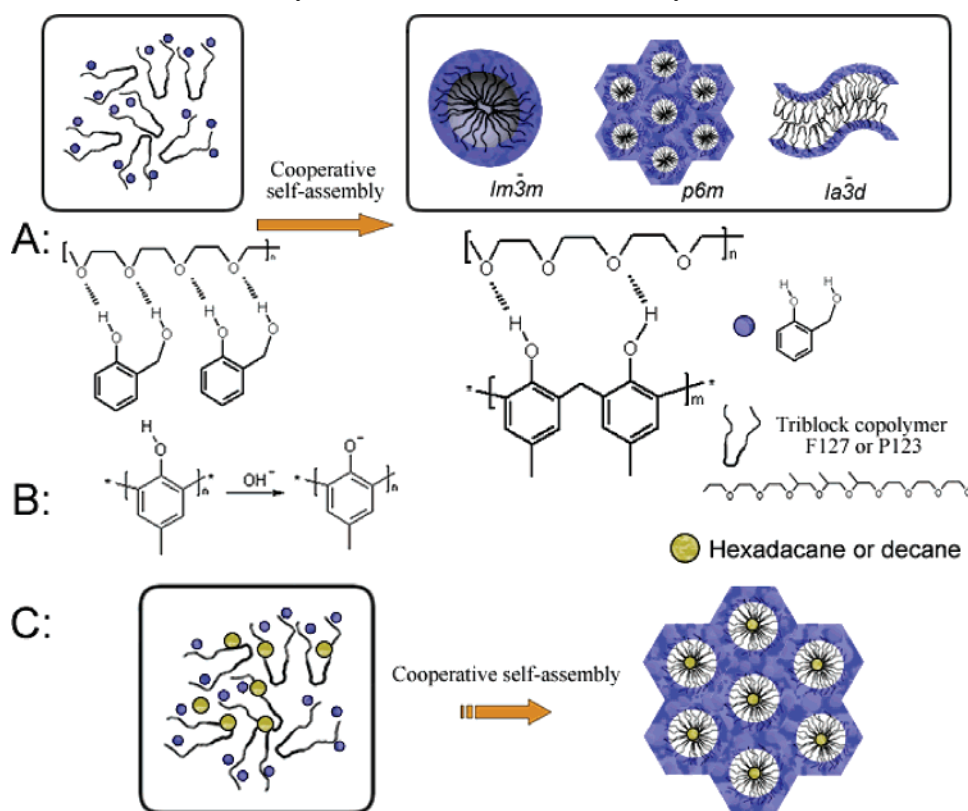
with a little better regularity on the millimeter scale (3–5 mm). After calcination at 350 and 800 °C, the size of the pellets became smaller because of the shrinkage, and no obvious cracking was observed. The average size of the pellets for FDU-15-C₁₆-350 and FDU-15-C₁₆-800 is 2–4 and 1–3 mm with shrinkage of about 30 and 50%, respectively. It is interesting that this shrinkage (50–60%) after calcination at 800 °C is a lot larger than that of the framework (32–34%), implying that many apertures exist. However, FDU-16 prepared using copolymer F127 as a template in aqueous solution shows quite different morphologies of rods and particles on the micrometer scale (Figure 15). The morphology of FDU-16 is varied by tuning the F127/phenol ratio. When the molar ratio is as low as 0.035, the SEM image shows that as-made FDU-16 is mainly composed of long rods 100–200 μm in length and 10–30 μm in width (Figure 15A). When the ratio increases to 0.040, the obtained FDU-16 shows a mixed morphology of rods and particles of ~10 μm (Figure 15B). The percentage of rods in the FDU-16 products decreases dramatically with increasing F127/phenol ratio. Only irregular spherulike particles ~5 μm in size can

be observed in the SEM image (Figure 15C) when the ratio increases to 0.048. These results suggest that the particle size decreases as the F127/phenol ratio increases.

Discussion

Formation. A simple aqueous solution route is employed here for the preparation of mesoporous carbon materials with hexagonal or cubic structure. The present aqueous approach is convenient, reproducible, and not limited by the batch size. The formation of the mesostructure is related to a possible cooperative self-assembly as shown in Scheme 1. Under a basic condition, phenol and formaldehyde can polymerize to low polymerization degree resols. The resols with abundant hydroxyl OH groups may interact with PEO segments of triblock copolymer through one-layer hydrogen bonds, further assembling the mesostructure of resols and triblock copolymers.²⁵ During the assembly, the phenolic resols may cooperatively polymerize around amphiphilic triblock copolymer micelles similar to the case of mesoporous silicates, further leading to the formation of large-sized particles with phenolic resin/triblock copolymer composites. The resins composed with three- or four-connected thermostet rigid frameworks are stable during the removal of triblock copolymers and can be transformed to mesoporous carbon after calcination at high temperature. The phenol/NaOH ratio is a key issue for the cooperative assembly of ordered mesostructures. When the phenol/NaOH molar ratio is higher than 8.4, the polymerization of resols is too slow to form mesoporous polymers. When the phenol/NaOH molar ratio is lower than 2.1, a relatively strong basic

Scheme 1. (A) A Possible Formation Mechanism of Mesoporous Polymers with a Variety of Structures in an Aqueous Solution under Basic Conditions, (B) Resol Anions Formed at a Relatively Strong Basic Condition, and (C) a Pore Size Swelling Process of Hydrocarbon Molecules in the P123 System



condition, resols may form as anions (Scheme 1B), which may weaken the hydrogen-bonding interaction between resols and triblock copolymer and result in the formation of a disordered mesostructure. Our results showed that a phenol/NaOH molar ratio of 4.2 with a pH value of ~ 9.0 is the optimal condition.

Mesostructures. Like the synthesis of mesoporous silicates under hydrothermal conditions, the formation of the mesostructure in our system is mainly dependent on the hydrophilic/hydrophobic interfacial curvature. Commonly, triblock copolymer with large PEO blocks may lead to the formation of a cubic mesophase with a high interface curvature. Thus, it is easily understood that Pluronic F127 induced the formation of the body-centered cubic $Im\bar{3}m$ mesostructure FDU-16 with high curvature. On the other hand, when Pluronic P123 with a small hydrophilic PEO segment is used as a template, a bicontinuous cubic mesophase (FDU-14, $Ia\bar{3}d$) with low interface curvature can be formed. Moreover, a phase transition from $Ia\bar{3}d$ to $p6m$ is observed with a decrease of the P123/phenol molar ratio or addition of hydrocarbon molecules. Hydrophilic resols can interact with PEO segments, while the hydrocarbon molecule, such as hexadecane, is hydrophobic and can interact with PPO segments. When the P123/phenol ratio increases, the hydrophilic/hydrophobic volume ratio in this system may decrease and the interface curvature may decrease to minimize the energy. As a result, a phase transition from $p6m$ to $Ia\bar{3}d$ occurs. Hexadecane and decane may swell the hydrophobic segment and increase the micelle size, so more resols may interact with PEO segments. As a result, both the hydrophilic and hydrophobic volumes increase, and a balance is reached, inducing the formation of a mesostructure (FDU-15) of pure $p6m$ symmetry. In addition, the pore size of FDU-15 can be tuned up to ~ 6.8 nm by adding hydrocarbon molecules.

Morphology. The morphology of mesoporous products is greatly influenced by the PEO/PPO ratio and the concentration of triblock copolymer, and this may be related to the interface of the polymerization/condensation. In the aqueous synthesis system, the polymerization/condensation rate of the resols is very slow at ~ 65 °C; it takes about 24 h to obtain phenolic resin/triblock copolymer sediments. The obtained sediment is of low polymerization degree with small sizes. Thus, when the reaction is prolonged, the sediment may further polymerize and aggregate to particles on the millimeter or/and micrometer scales as a result. When triblock copolymer P123 with a lower PEO/PPO ratio is used as a template, the interface may be more hydrophobic compared with that in the case of F127, resulting in easy aggregation

of particles and pellet-like morphologies with larger sizes (1–5 μm). During synthesis of FDU-16, the initial amount of F127 is far beyond that in the final products. The excess triblock copolymer F127 with a high PEO/PPO ratio in the solution may cover the surface of small sediments formed at the beginning through the hydrogen-bonding interaction. This may inhibit further aggregation of small sediments, resulting in particles with sizes on the micrometer scale. When the F127 concentration increases, sediments can be further dispersed in the solution, resulting in a decrease of the particle size of FDU-16.

Conclusion

We have demonstrated a simple and reproducible aqueous approach for the synthesis of mesoporous polymers or carbons with a variety of structures ($Im\bar{3}m$, $p6m$, and $Ia\bar{3}d$) and morphologies by using triblock copolymers as templates and resols as carbon sources under basic conditions. Hydrocarbon molecules such as hexadecane or decane can be used as swelling agents to tailor the pore sizes (4.1–6.8 nm) and mesostructures. Highly ordered mesoporous carbon materials with body-centered cubic $Im\bar{3}m$ structure (FDU-16) can be synthesized by using triblock copolymer F127 as a template at a relatively wide range. With addition of hydrocarbon molecules, ordered mesoporous carbons with 2-D hexagonal $p6m$ structure (FDU-15) have been obtained in the aqueous synthesis process for the first time. A short-chain hydrocarbon such as decane may have a strong interaction with the PPO segment of amphiphilic triblock copolymers and yield a large pore size. Using P123 as template, a phase transition from $Ia\bar{3}d$ to $p6m$ occurs as the molar ratio of P123/phenol decreases from 0.040 to 0.026. A one-layer hydrogen bond interaction induced cooperative assembly mechanism is proposed for the aqueous synthesis route. Moreover, the morphology and particle size can be controlled by varying the PEO/PPO ratio and concentration of triblock copolymers. Mesoporous carbon materials with a pellet-like morphology in the size range of 1–5 μm and a rodlike particle morphology in the size range of 5–200 μm were obtained.

Acknowledgment. This work was supported by the NSF of China (Grants 20233030, 20421303, 20373013, and 20521140450), the State Key Basic Research Program of the PRC (Grant 2001CB610506), the Shanghai Science & Technology Committee (Grants 04JC14087, 055207078, and 05DZ22313), the Program for New Century Excellent Talents in University (Grant NCET-04-03), the LG Co., the Shanghai HuaYi Chemical Group, and Fudan Graduate Innovation Funds. We greatly thank Dr. Y. Chen, Dr. S. H. Xie, and Dr. L. J. Zhang for experimental and characterization assistance.